Conductive Polymer Film-Based $BaTiO_3$ Strain Sensors for Flexible Applications

[1*]Priya Gupta, [2]Praveen Patidar
[1]MTech Student, [2]Head of Department
[1,2]Department of Electrical and Electronics Engineering,
[1,2]Lakshmi Narain College of Technology and Science, Indore, India.

Abstract: Conducting polymer nanocomposites find applications in various flexible sensing applications and analyte-recognizing element biosensors. There is a growing demand for conductive stretchable materials to be used as strain sensors, with widespread attention due to the ease of processing with the stretchable polymer matrix and conductive nanoparticles. They benefit with high flexibility, good stretchability, excellent durability, tune able strain sensing behaviors. This article reports the use of LDPE as a base-matrix for modified polymer nanocomposite based stretchable sensor with $BaTiO_3$ nanoparticles as the nano-inclusions. The proportions of $BaTiO_3$ is varied as 12% and 15% with weight of the base polymer matrix. The crystallinity varied with the increased proportions of the nanoparticles as 34.9 % and 34.4 % for 12% and 15% samples respectively, and the maximum electrical polarization response was observed to change from 0.00049 C/mm^2 to 0.00337 C/mm^2 between Pure LDPE and 12% sample but very minimal difference between 12% and 15% sample. The maximum polarization, remnant polarization and coercive field, all increased with the increasing nano-inclusion loading. The results suggest the suitability of such film-based strain sensors for commercial applications and the method is easily scalable too.

Keywords **- Composites; Thermoplastic; LDPE; Flexible sensor, Strain.**

I. INTRODUCTION

Conductive polymers are attracting much attention for varieties of applications, due to their ease of processing and the prospects of multiple bespoke properties inclusion [1]. Since, the brittle ferroelectric ceramics cannot be used for flexible applications, though having extraordinary dielectric behavior. And on the other hand, polymers are very flexible and easy to process but have high dielectric breakdown field. The composite conductive polymers utilize the best trait of each by combining them both and forming a material that is flexible and suitable for applications into electronic devices for achieving high volume efficiency [2]. One category of these conductive polymers is based on the interconversion of electrical and mechanical energies, viz. piezoelectric effect. Such materials are finding applications into energy harvesting, transducer, actuator, etc. Popular areas of applications are summarized in Fig. 1. Some application examples are automated fuel injection actuators, ink-jet printers, transducers used in ultrasonic imaging, vibration-controlled sensors, sonars, etc.

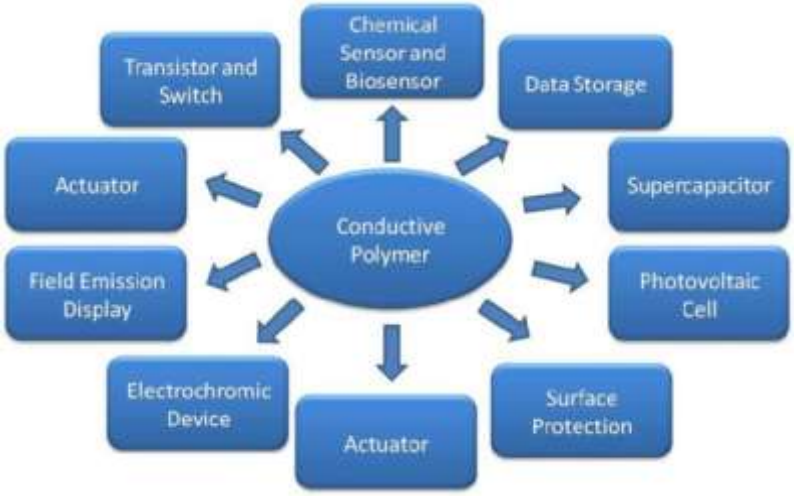

Figure 1. Various application areas of conductive polymer composites [3].

Though the realization of such composite materials for many applications, like interactive robotics and wearable devices, demand light and flexible materials, which is still a challenge. Above that these applications demand materials with tuneable electrical conductivity, large surface areas, light weight along with superior mechanical stability and at the same time easier to manufacture with minimum processing cost. This is where the nanocomposite conducting polymers involving the piezoelectric nanoparticles (NPs) as the inclusions in the base polymer matrix, can serve exactly as desired. The large surface-to-volume ratio of the nanoparticles aids in addressing all the listed qualities [4-8] for flexible application.

But the assured benefits with the nano-inclusions can only be attained, if the nanoparticles are dispersed uniformly in the polymer matrix, which is easier said than done. The NPs tend to agglomerate due to their dipole-dipole interaction [6], and when introduced in a viscous melt polymer it becomes even difficult to disperse them uniformly. If not addressed properly, such issues can lead to agglomerates in the nanocomposite leading to local charge accumulation and non-uniform electrical or heat conduction [7]. The agglomeration issue can be minimized by various techniques, of which functionalization of NPs is the most effective one [6]. Functionalization involves coating the individual NP with a suitable chemical moiety that fits in conjunction or much suitability with the base polymer chains. The functionalization can serve two purposes, i.e. firstly to reduce the interparticle attraction between

the NPs and secondly to align the NPs hierarchically within the base polymer chain lengths, depending on the functional groups interacting.

Hence, as a general recommendation functionalized NPs are to be used for nanocomposite synthesis. In particular, in this study we used silica functionalized Barium Titanate (BT) NPs, which are proven to improve dispersion as compared to the uncoated NPs [9], to prepare the BT-LDPE conducting polymer (CP) nanocomposites. Though this dielectric metal oxide-based CP was prepared with varying weight percentage proportions of the NPs, to characterize the resulting effect on the dielectric phenomenon and to assess their suitability for strain measurement.

II. EXPERIMENTAL SECTION

2.1 Materials

Low Density Polyethylene (LDPE) granules with 2 g/10 min melt flow rate (920 Kg/m^3) was purchased from Goodfellow (UK). Barium Titanate ($BaTiO_3$) nanoparticles (< 50 nm size) (BET), 90% technical grade Tetraethyl Orthosilicate (TEOS), Cis-cyclooctene containing 100-200 ppm Irganox 1076 FD as antioxidant, Citric acid 99% and anhydrous 99% Heptane were all used as received from Sigma Aldrich (UK). Other laboratory agents were used as standard. Throughout the experiment, deionized water with 18 MO conductivity was used.

2.2 Experimental Method

The BT NPs were functionalized/coated as per the following procedures. The pre-treatment of BT NPs was done by dispersing 500 mg of NPs in 10 mL of 1M HNO_3 and mixed vigorously by ultra-sonication for 5 mins; this acidic treatment activated the NPs surfaces. Supernatant was discarded by centrifuging at 4500 rpm and the NPs were subsequently washed for three times with deionized water after every centrifuge. The collected NPs were then dispersed in 10 mL of 0.01 M citric acid solution and mixed under ultra-sonication for 5 mins; absorption of citric acid will enhance the colloidal stability in alcohol based aqueous reacting medium, promoting the silica functionalization of NPs. Excess acid was discarded by centrifuging at 4500 rpm, followed by deionized water washing and repeated three times. The collected NPs were then dispersed in 20 ml water solution containing 20 µL ammonia and left for 24 Hrs. The silica coating procedure then implemented by dispersing these citrated BT NPs in 100 mL of ethanol/water/ammonia solution with 75/23.5/1.5 % volume proportion of each, respectively. 55.5 – 111 µL of TEOS was then slowly introduced in this solution to form ca. 2 - 4 µm thick silica coatings on the NPs. The mixture was left under magnetic bar stirring for overnight at room temperature; this initiated the hydrolysis and condensation of TEOS to form silica shells around the NPs. The silica coated NPs were then recovered by centrifuging the mixture three times at 5000 rpm for 8 minutes, followed by ethanol washing each time. The collected BT NPs were then sintered for three hours, with a gradual rise in temperature and finally maintained at 1000 ˚C. Similar, procedure was followed to prepare the required quantity of functionalized NPs for making the complete batch of nanocomposite samples.

The nanocomposite films were then prepared by using Twin-tech 10 mm twin-screw extruder. 12 wt% of functionalized BT NPs was mixed with 15 g of LDPE along with 0.5 ml cis-cyclooctene. The inclusion of cis-cyclooctene prevented oxidation of LDPE during the extrusion process. All the regions of the extruder were maintained at 140 °C temperature and the screw speed were set to 60 rpm, for uniform feed. To improve the dispersibility of the NPs, each sample was extruded two times. The resulting nanocomposite films were of 80-150 µm thickness. Similarly, other sample with 15 wt% of NPs was prepared. The samples are here onwards referred as 12% and 15% samples.

2.3 Characterization Techniques

Attenuated Total Reflection spectra (ATR-FTIR) were recorded on Perkin-Elmer make, using DGS-KBr sensor for identifying the effect with silica functionalization of nanoparticles. Nanocomposite films were characterized with a total of 30 scans in each run and within the range of 525–4000 cm^{-1} wavenumber with a resolution of 4cm^{-1}; to identify functional groups and structural changes after the addition of nanoparticles.

Differential scanning calorimetry (DSC) was done using TA Instruments DSC Q100 and TGA Q500 with a sample mass of 7-12 mg. The Heat/Cool/Heat standard cycle type analysis was selected for accurately depicting the Tm for each sample. The selected cycle consisted of a ramp heating at 10 °C/min from 25 to 150 °C, then ramp cooling at 5 °C/min to -50 °C followed by ramp heating at 10 °C/min to 150 °C.

The hysteresis loops were plotted as polarization vs. electric field (P-E) and strain vs. electric field (S-E) measurements were obtained by using aixACCT systems GmbH Germany, an advanced ferroelectric test system having a piezo sample holder unit (PSHU) connected with a high voltage 28 kV amplifier. The direction of application of the electric field and the direction of displacement (measurement) were maintained same.

III. RESULTS AND DISCUSSIONS

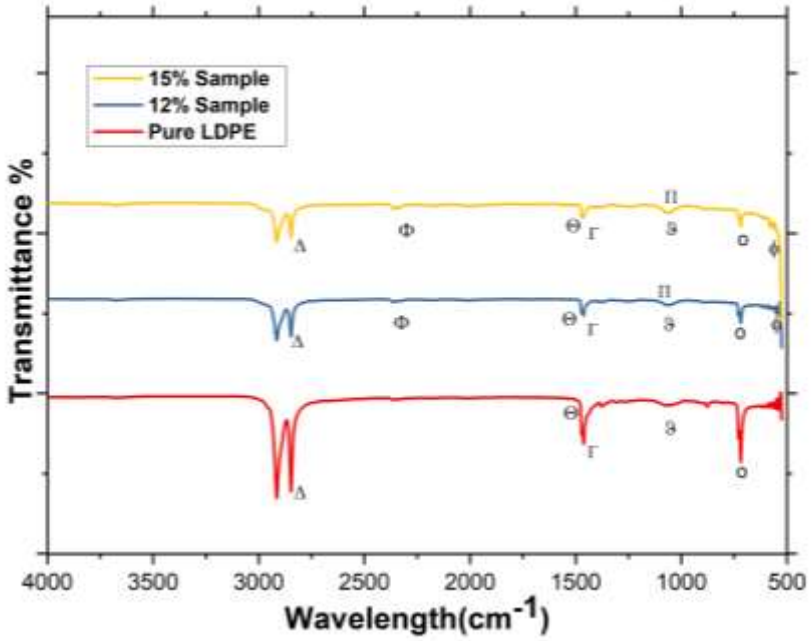

Figure 2. FTIR spectra of Pure LDPE and the prepared 12% and 15% nanocomposite samples.

The IR spectra gives an idea on the effect of the NPs inclusion on the LDPE matrix and also hints towards the crystallinity induced properties; of which the one's related to this study are charge carrying capacity and mechanical stability. Fig. 2 highlights the LDPE backbone peaks with -CH_2 stretching band around 2911-2916 cm^{-1} and the -CH_3 stretching band around 2839-2849 cm^{-1} (Δ) [4] however, these peaks are somewhat suppressed by the presence of silica functionalization. Other representative peaks of ν(C=O), δ(C-H), γ(=C-H) and γ(C-H) are subsequently seen at around 1450 cm^{-1} (Θ), 1460 cm-1 (Γ), 1030 cm^{-1} (ϑ) and 710 cm^{-1} (o) respectively [4]. The NP-bulk absorption (709-725 cm^{-1}) [10] and minor peaks around 714-719 cm^{-1} are due to the Si–O stretching of SiOH [11], whereas the peak around 862 cm^{-1} is due to hydroxyl (OH) group of the adsorbed H_2O [12]. The $BaCO_3$ (Φ) and TiO (φ) bonds from the $BaTiO_3$ NPs are observed around 2260 cm^{-1} and 530 cm^{-1} respectively [7]. Reduced polymer chain mobility causes slow crystal formation and hence resulting in higher degree of crystallinity [coco]. Though the IR spectra does not give an exact estimation of the crystallinity value, hence the DSC as a suitable tool was followed for this estimation.

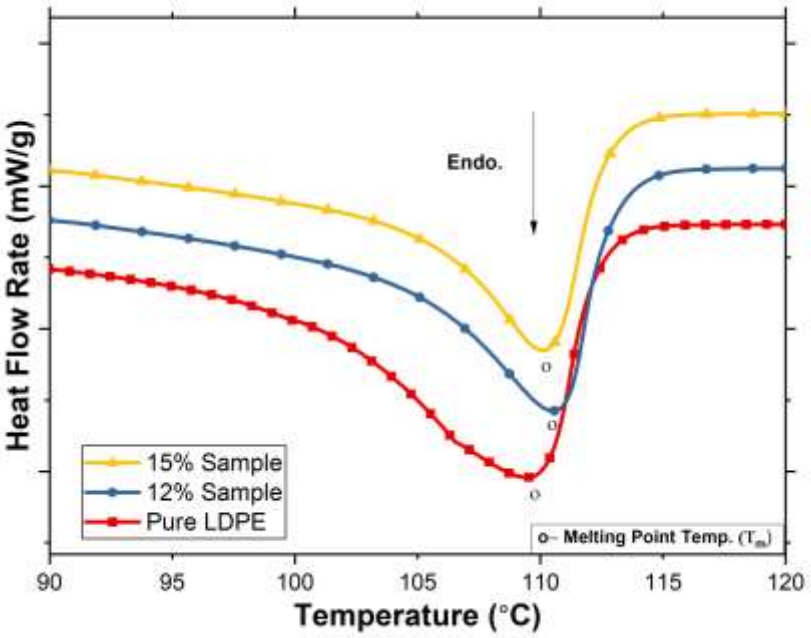

Figure 3. DSC melting endothermic peaks used for crystallinity calculation for Pure LDPE and the prepared 12% and 15% nanocomposite samples.

The degree of crystallinity dictates the suitability of the nanocomposite material for film formability and its application in structural areas [5,13]. In DSC study, the variations associated with ranging crystal sizes and crystal defects are identified with variations in endothermic transition energy absorbed during the sample melting phenomenon. From Fig. 3 its observed that the melting temperature (T_m) decreases with the increased NP loading and is as expected with the introduced dielectric filler impurities

that have higher thermal and electrical affinity [4]. The degree of crystallinity of all samples was calculated as listed in Table 1, taking melting heat of completely crystallized polyethylene as 286.7 J/g [4].

Table 1. Melting temperature (T_m) and degree of crystallinity from DSC results for Pure LDPE, 12% and 15% nanocomposite samples.

Sample	**T_m** (°C)	**Enthalpy** (J/g)	**Degree of Crystallinity** (%)
Pure LDPE	109.46 ± 1	110.46 ± 1	38.53 ± 1
12% Sample	110.24 ±1	100.10 ± 1	34.92 ± 1
15% Sample	109.82 ± 1	98.63 ± 1	34.40 ± 1

The decreasing trend of degree of crystallinity with the increasing NP loading is due to nucleating sites formed by the NPs inclusion, which also resulted in Tm reduction. Though the reduction is not drastic enough, to adversely affect the mechanical stability due to the NPs inclusion. This confirms that the synthesized samples can be very well formed into film samples, without any signs of brittle wear as expected by bulk $BaTiO_3$ ceramic materials or even bulk piezoelectric composites.

Figure 4 shows the P-E hysteresis loops for Pure LDPE, 12% and 15% nanocomposite samples. The maximum electric field strength conducted by each sample of Pure LDPE, 12% and 15% NP variations was 28 mV/mm, 188.15 mV/mm, and 206 mV/mm, respectively. The increasing conduction is directly proportional with the dielectric content of the NPs present, hence proving the improvements with the NPs inclusion.

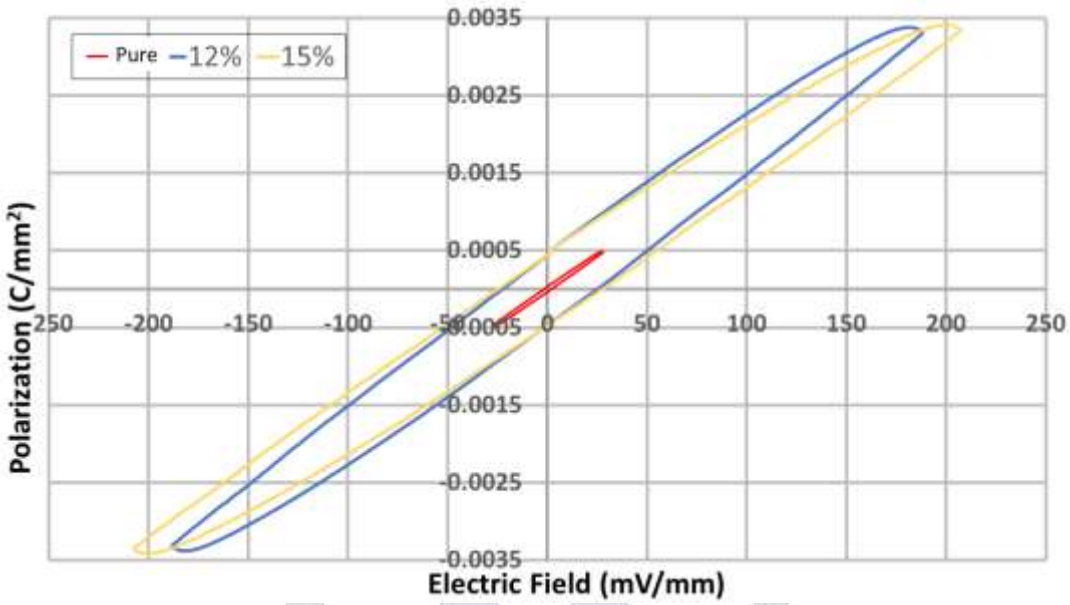

Figure 4. Polarization versus electric field (P-E) hysteresis loops for Pure LDPE and the prepared 12% and 15% nanocomposite samples.

The increase in P_{max} is primarily due to the inclusion of piezoelectric BT NPs, which possibly caused the decrease in cell volume of the doped conductive composites. Also, as the wt% of the NPs increases there is a possibility of some reduction in polarization per unit cell due to the random orientations of the local polar domains [14]. This could be the possible reason why there is not a much difference observed in the P_{max} of 12% and 15% samples. Further, from Table 2 its observed that the coercive field E_c and remnant polarization P_r are observed to decrease as the NP concentration increases from Pure LDPE to 15%. This is in line with the response as observed with P_{max}.

Table 2. Maximum polarization P_{max}, remnant polarization P_r and coercive field E_c for Pure LDPE, 12% and 15% nanocomposite samples.

Sample	**P_{max}** (C/mm^2)	**P_r** (C/mm^2)	**E_c** (mV/mm)	**P_r/ P_{max}**
Pure LDPE	0.00049	0.000041	2.2014	0.0837
12% Sample	0.00337	0.00044	25.505	0.1306
15% Sample	0.00341	0.00045	27.221	0.1319

With the P-E results its observed that the hysteresis loop parameters (P_{max}, P_r, and E_c) increase with the increasing nano inclusions of BT NPs. Hence concluding that the higher amount of NP loading led to an increased strength of polarization with applied electric field in the synthesized conductive film samples. This property is much desired for any sensing capability [15].

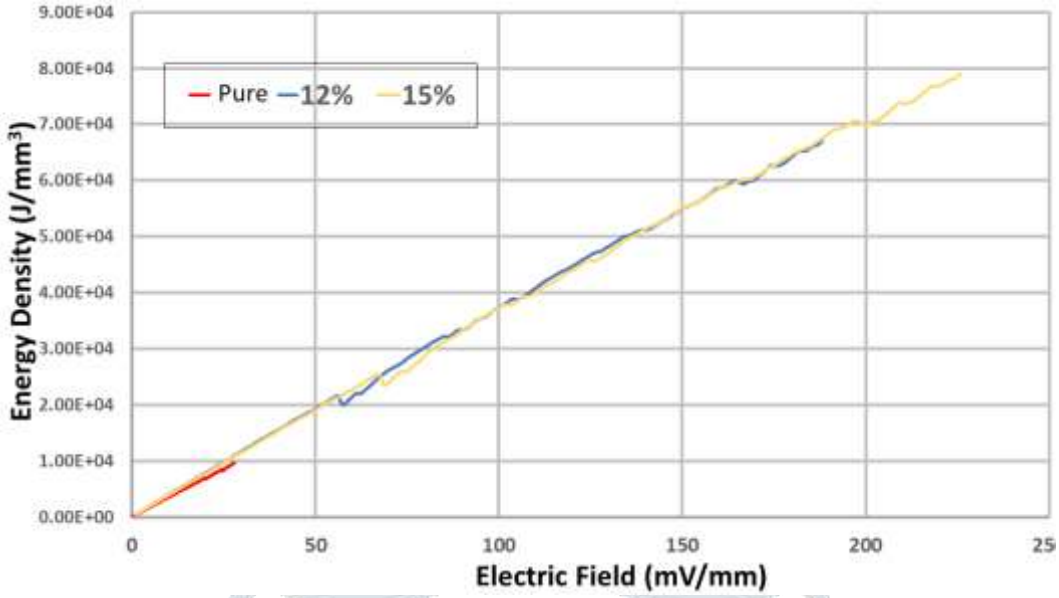

Figure 5. Resistance (strain) versus electric field (S-E) measurements for Pure LDPE and the prepared 12% and 15% nanocomposite samples.

Further the changes in impedance of the prepared piezoelectric thin film samples was studied due to applied electric field. Fig. 5 depicts the trend of increasing resistance with the increase of applied electric field as observed in previous studies with BT crystals [2]. When the film samples are subjected to the increasing electric field, they experience tensile loading due to the virtue of the piezoelectric nature of the BT crystals present as NPs within them. The films hence show an increase in strain and a corresponding increase in resistance as recorded with the increase in NPs loading. The sample with 12% and 15% NPs loading showed a huge difference in the impedance values as compared to the Pure LDPE sample; similar response was also observed in the P-E measurements. As we know that LDPE being an insulator itself does has a tendency for leakage current, when subjected to maximum applied electric field. But due to the BT nano inclusions it also starts exhibiting domain switching. Interestingly, after a certain limit of the NPs loading domain switching becomes prominent and causes the induced peak current to surpass the magnitude of the leakage current caused at the maximum applied electric field [15]. Hence, the increased BT NPs loading can be justified as susceptibly be the cause of enhancing the response between the Pure LDPE and 12% or 15% samples as recorded in the P-E and impedance measurements.

IV. CONCLUCIONS

The dielectric $BaTiO_3$ nanocomposite samples were prepared with 12% and 15% weight loading of NPs and were formed into 80-150 μm thick films and characterized. FTIR results highlighted the LDPE backbone modifications and the effect due to silica coating with $BaTiO_3$ NPs inclusion was observed. Further the DSC results gave a clear estimation of the melting temperature and the degree of crystallinity, both were observed to drop with the increased NPs loading in the samples. The crystallinity of 12% and 15% samples did not modify much, from that of the Pure LDPE. This suggests that the nano-inclusions brought in improvements of dielectric nature, but the mechanical ability and thermal stability needed for thin film processing and strength requirements for structural applications were still maintained.

The polarization vs. electric field (P-E) measurement showed a maximum polarization (P_{max}) and coercive field (E_c) between Pure LDPE and 12% (or 15%) samples. Further the impedance (strain) vs. electric field (S-E) measurements confirmed the strain sensing capability of the prepared samples, by showing increasing impedance with the increase of applied electric field. Our results demonstrate the sensitivity and robust operational range of these flexible sensors for a range of industrial applications.

ACKNOWLEDGMENT

The authors are very grateful and thankful to the support of Dr. Ketan Pancholi and Dr. Ranjeetkumar Gupta of Robert Gordon University, UK; for their invaluable support in helping to characterize the samples and make meaningful conclusions.

REFERENCES

[1] Bai, Y.; Cheng, Z.; Bharti, V.; Xu, H.; Zhang, Q. High-dielectric-constant ceramic-powder polymer composites. *Appl Phys Lett* **2000**, *76*, 3804-3806.

[2] Baraskar, B.G.; Kadhane, P.S.; Darvade, T.C.; James, A.R.; Kambale, R.C. BaTiO3-Based Lead-Free Electroceramics with Their Ferroelectric and Piezoelectric Properties Tuned by Ca2, Sn4 and Zr4 Substitution Useful for Electrostrictive Device Application. *Ferroelectrics and their applications* **2018**, 113.

[3] Brillians Revin, S., Electrochemical sensors for biomolecules using functionalized triazole modified conducting polymer electrodes. (Doctoral dissertation, Gandhigram Rural Institute). 2012.

[4] Gupta, R.; Smith, L.; Njuguna, J.; Deighton, A.; Pancholi, K. Insulating MgO-Al2O3-LDPE Nanocomposites for Offshore Medium Voltage DC Cable. *ACS Applied Electronic Materials* **2020**, *2*, 1880-1891.

[5] Gupta, R.; Huo, D.; White, M.; Jha, V.; Stenning, G.B.; Pancholi, K. Novel Method of Healing the Fibre Reinforced Thermoplastic Composite: A Potential Model for Offshore Applications. *Composites Communications* **2019**, *16*, 67-78.

[6] Gupta, R.; Pancholi, K.; De, S., Rulston; Murray, D.; Huo, D.; Droubi, G.; White, M.; Njuguna, J. Effect of Oleic Acid functionalised Iron Oxide Nanoparticles on Properties of Magnetic Polyamide-6 Nanocomposite *The Journal of The Minerals, Metals & Materials Society (TMS)* **2019**, *71*, 3119-3128.

[7] Gupta, R.; Huo, D.; Pancholi, M.; Njuguna, J.; Pancholi, K. Insulating polymer nanocomposites for high thermal conduction and fire retarding applications. In the proceedings of the 3rd Defence & Security Doctoral Symposium 2017, Cranfield Unviersity: 2017.

[8] Gupta, R.; Pancholi, K.; Prabhu, R.; Pancholi, M.; Huo, D.; Jha, V.; Latto, J. Integrated self-healing of the composite offshore structures, OCEANS 2017-Aberdeen, IEEE: 2017; pp. 1-4.

[9] Mornet, S.; Elissalde, C.; Hornebecq, V.; Bidault, O.; Duguet, E.; Brisson, A.; Maglione, M. Controlled growth of silica shell on Ba0. 6Sr0. 4TiO3 nanoparticles used as precursors of ferroelectric composites. *Chemistry of materials* **2005**, *17*, 4530-4536.

[10] Cornu, D.; Guesmi, H.; Krafft, J.; Lauron-Pernot, H. Lewis acido-basic interactions between CO2 and MgO surface: DFT and DRIFT approaches. *The Journal of Physical Chemistry C* **2012**, *116*, 6645-6654.

[11] Larkin, P. IR and Raman spectra—Structure Correlations: Characteristic Group Frequencies. *Infrared and Raman spectroscopy* **2011**, 73-115.

[12] Prescott, H.A.; Li, Z.; Kemnitz, E.; Deutsch, J.; Lieske, H. New magnesium oxide fluorides with hydroxy groups as catalysts for Michael additions. *Journal of Materials Chemistry* **2005**, *15*, 4616-4628.

[13] Gupta, R.; Staknevicius, R.; Pancholi, K. Rapid Multifunctional Composite Part Manufacturing using Controlled In-situ Polymerization of PA6 Nanocomposite. *Procedia CIRP* **2019**, *85*, 61-65.

[14] Kshirsagar, S.H.; Tarale, A.N.; Jigajeni, S.R.; Salunkhe, D.J.; Joshi, P.B. Effect of Ni doping on ferroelectric, dielectric and magneto dielectric properties of strontium barium niobate ceramics. *Indian Journal of Pure & Applied Physics (IJPAP)* **2015**, *53*, 119-124.

[15] Kumar, A.; Prasad, V.B.; Raju, K.J.; James, A. Optimization of poling parameters of mechanically processed PLZT 8/60/40 ceramics based on dielectric and piezoelectric studies. *The European Physical Journal B* **2015**, *88*, 287.